ORIGINAL ARTICLE

Physiological background parenchymal uptake of ^{18}F-FDG in normal breast tissues using dedicated breast PET: correlation with mammographic breast composition, menopausal status, and menstrual cycle

Yuri Shimizu[1] · Hiroko Satake[1] · Satoko Ishigaki[1] · Kazuhiro Shimamoto[2] · Fuga Uota[1] · Masanori Tadokoro[3] · Tomohiro Sato[3] · Katsuhiko Kato[4] · Tsuneo Ishiguchi[3] · Shinji Naganawa[1]

Abstract

Objective This study aimed to quantitatively evaluate the effects of age, mammographic density, menopausal status, and menstrual cycle on background parenchymal uptake (BPU) using ring-shaped dedicated breast positron emission tomography (dbPET).

Methods This study included 186 adult women who underwent mammography and dbPET on the same day and had no abnormalities classified as Breast Imaging Reporting and Data System (BI-RADS) category 1 on both examinations. The volume of interest (VOI) was placed in the glandular tissue of both breasts, and the maximum standardized uptake value (SUV_{max}), mean standardized uptake value (SUV_{mean}), and metabolic breast volume (MBV) were measured as indicators of BPU. We analyzed the correlation between BPU and age, mammographic density, menopausal status, and menstrual cycle.

Results The SUV_{max} and SUV_{mean} for normal breast tissue were inversely correlated with age (both $p < 0.001$). The SUV_{max}, SUV_{mean}, and MBV of mammographically dense breast tissues were significantly higher than those of non-dense breast tissues (all $p < 0.001$). The SUV_{max}, SUV_{mean}, and MBV of normal breast tissue in premenopausal women were significantly higher than those in postmenopausal women ($p < 0.001$, $p < 0.001$, $p = 0.002$, respectively). In the study, 59 premenopausal women, the SUV_{max} of normal breast tissue in the menstrual-follicular phase was significantly lower than that in the periovulatory-luteal phase ($p = 0.02$). When we sorted the premenopausal women by mammographic breast composition, the SUV_{max} and SUV_{mean} of normal breast tissues in the menstrual-follicular phase were significantly lower than those in the periovulatory-luteal phase in the 44 premenopausal women with dense breasts ($p = 0.007$, and $p = 0.038$, respectively), whereas no statistically significant difference was found between the menstrual-follicular phase and the periovulatory-luteal phase in the 15 premenopausal women with non-dense breasts.

Conclusions BPU in normal breast tissues assessed using ring-shaped dbPET was associated with mammographic density, menopausal status, and women's menstrual cycle. The menstrual cycle was significantly associated with BPU in premenopausal women with dense breasts but not in women with non-dense breasts.

Keywords Breast · PET · Dedicated breast positron emission tomography · Menstrual cycle · Beast density

Introduction

^{18}F-fluorodeoxyglucose (FDG) is widely used to detect malignant tumors. In breast cancer treatment, whole-body positron emission tomography (PET) is primarily used to search for systemic metastasis and to determine chemotherapeutic effects; however, it has limited detection of breast cancer due to low spatial resolution. In recent years, high-resolution dedicated breast PET (dbPET) scanners have been developed to detect small breast lesions. There are two types of dbPET scanner: positron emission mammography (PEM) and ring-shaped dbPET. Researchers have reported that these systems show improved resolution and detectability of small lesions by setting the detector close to the breast

✉ Satoko Ishigaki
satoko@med.nagoya-u.ac.jp

Extended author information available on the last page of the article

tissue and using smaller detection units than whole-body PET [1–3]. Ring-shaped dbPET is being increasingly used compared with PEM because it is painless, as it only hangs the breast into the detector, unlike PEM, which requires compression of the breast by the detector. Furthermore, the inspection time of ring-shaped dbPET is shorter than that of PEM, and the standardized uptake value (SUV) can be easily measured with imaging modality.

Increased FDG uptake is observed in breast cancers, while mild physiological uptake is observed in the background of normal breast tissues. It is hypothesized that the intensity of physiological FDG uptake in the background breast parenchyma affects the detectability of breast cancer on PET. In whole-body PET, several studies have reported that FDG uptake in the background parenchyma of normal breast tissues can vary with age, mammographic density, menopausal status, and menstrual cycle [4–9]. However, in dbPET, only one study has compared the degree of FDG uptake in background breast tissues with age, mammographic density, and menopausal state using PEM [10]. As far as we know, there have been no studies which have examined the association of the menstrual cycle with background parenchymal FDG uptake using dbPET. Clarifying this relationship may lead to improved diagnostic accuracy of breast cancer by optimizing the subjects in screening tests using dbPET and adjusting the imaging schedule according to patients' menstrual cycle.

Therefore, we examined the effects of age, mammographic density, menopausal status, and menstrual cycle on background parenchymal uptake (BPU) in normal breast tissues using ring-shaped dbPET.

Methods and materials

Study population

We retrospectively reviewed the imaging data of adult women who underwent breast cancer screening at a single medical center between April and September 2017. We selected a total of 213 adult women who underwent mammography and dbPET on the same day and had no abnormalities classified as Breast Imaging Reporting and Data System (BI-RADS) category 1 on both examinations. All participants completed a questionnaire on the day of their mammography and dbPET. We asked participants whether they were premenopausal or postmenopausal. For the women who were premenopausal, the first day of the last menstrual period, cycle length, and regularity of their menstrual cycles were asked, and this information was recorded.

We excluded 22 premenopausal women who did not remember their last normal menstrual period or who had irregular menstrual cycles, 1 woman who had previously received treatment for a breast mass, 2 women with blood glucose levels over 150 mg/dl, and 2 postmenopausal women who were receiving hormone treatment. Finally, 186 women (mean age, 56.3 ± 11.8 years; age range, 28–79 years) were included; of these, 59 were premenopausal and 127 postmenopausal. None of the subjects were pregnant or lactating.

This retrospective study was approved by our institutional review board and complied with the ethical standards established in the 1964 Declaration of Helsinki and all subsequent revisions. The requirement for informed consent was waived.

Mammography

Digital mammography was conducted on Selenia Dimensions (Hologic, Bedford, MA, USA) to obtain standard mediolateral oblique (MLO) and craniocaudal (CC) views. A 5-megapixel monitor was used to read mammograms.

Mammograms were independently evaluated by two radiologists with 30 and 23 years of experience in breast imaging within 1 week of examination. Breast composition was categorized into four groups according to the BI-RADS classification as follows: almost entirely fat, scattered fibroglandular tissue, heterogeneously dense, or extremely dense. The radiologists determined BI-RADS scores ranging from 1 to 5 as follows: 1-negative, 2-benign findings, 3-probably benign, 4-suspicious abnormality, 5-highly suspicious for malignancy. The imaging results were finalized by consensus reporting and recorded.

dbPET scanning protocols

Participants fasted for at least 6 h before administration of ^{18}F-FDG (3 MBq/kg). Approximately 60 min after the injection, whole-body PET/CT (Discovery IQ, GE Healthcare, Milwaukee, WI, USA) was performed. After PET/CT scanning, approximately 85 min after injection, dbPET (Elmammo, Shimadzu, Kyoto, Japan) was performed for 5 min for each breast in the prone position. First, the right breast was scanned. The dbPET images were reconstructed with one iteration of a 3-dimensional list mode DRAMA (Dynamic Row-Action Maximum Likelihood Algorithm) and 128 subsets, a relaxation control parameter with a β value of 20, a matrix size in the axial view of $236 \times 200 \times 236$ with a post-reconstruction Gaussian smoothing filter (1.17 mm full width at half maximum), and a convolution-subtraction scatter correction. An attenuation correction was applied. Assuming that the breast was soft tissue not containing bone or air, this device estimated the breast contour from the measurement data and obtained an attenuation correction coefficient. The dbPET images were evaluated by the consensus of the same two radiologists who evaluated the mammograms within 1 week after the examinations. The absence of increase in focal or regional uptake

in comparison with the background on the whole glandular tissue of the bilateral breasts was defined as normal. Uptake near the boundary of the field of view (FOV) for the thoracic wall was diagnosed as image noise and was regarded as a normal finding.

Analysis of background parenchymal uptake on dbPET

As an indicator of BPU, the maximum standardized uptake value (SUV_{max}), mean standardized uptake value (SUV_{mean}), and metabolic breast volume (MBV) of the breast tissue were measured, and the average value of the two breasts was considered. One radiologist with 2 years of experience in general imaging, blinded to the menopausal status and mammographic findings of the women, analyzed the dbPET images at a workstation (Centricity Universal Viewer, GE Healthcare), providing multiplanar reconstruction images. First, a rectangular parallelepiped-shaped volume of interest (VOI) was manually placed, carefully enclosing the whole glandular breast tissue, in axial, coronal and sagittal images (Fig. 1). To avoid artifacts at the edge, this master VOI was placed more than 10-mm away from the image margin. The nipples were excluded. The SUV_{max} defined as the hottest voxel within the master VOI, was quantified. Then, the breast tissue was automatically segmented using an isocontour threshold method defined as 42% of the SUV_{max}. The SUV_{mean} was calculated as the average SUV of the voxels in the segmented VOI, and the MBV as the total volume of the voxels in the segmented VOI. As a threshold, we adopted a value of 42%, which was set in the workstation as a default based on a previous report [11].

Data collection

We collected data on participants' age and menopausal status from their medical records. For premenopausal women, the first day of the last menstrual period and the length of their menstrual cycles were also recorded. The menstrual cycle date at the time of the dbPET study was calculated from the reported last menstrual period and categorized as menstrual-follicular phase (days 1 – 12) or periovulatory-luteal phase (days $\geq$ 13). For women with menstrual periods longer or shorter than 28 days, the menstrual-follicular phase was defined as the period from the first day of menses to 2 days before the date of ovulation, which was estimated as 14 days before the first day of the next menstrual cycle.

Statistical analysis

We examined the relationship between BPU (SUV_{max}, SUV_{mean}, and MBV) and age, mammographic density, and menopausal status in 186 women. Mammographic density was classified as dense breast (heterogeneously dense and extremely dense) or non-dense breast (almost entirely fat and scattered fibroglandular tissue) based on the assigned breast compositions.

Spearman's rank correlation was used to assess the correlation between BPU and age. The Mann–Whitney U test was used to analyze the relationship between BPU and mammographic density, menopausal status, and the menstrual cycle. To identify independent predictors of BPU, stepwise multiple regression analysis was performed using age, mammographic density, menopausal status, and menstrual cycle as variables.
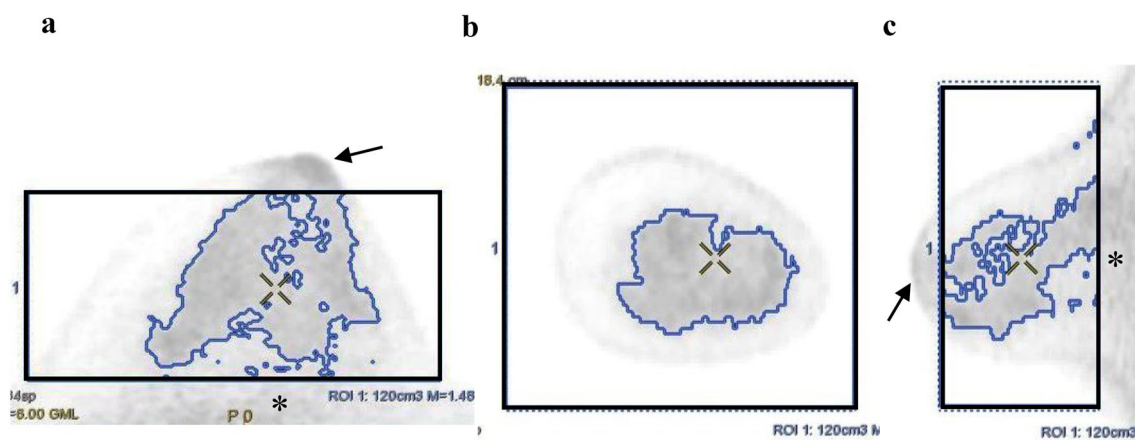

Fig. 1 Maximum standardized uptake value (SUV_{max}), mean standardized uptake value (SUV_{mean}), and metabolic breast volume (MBV) in the background parenchymal uptake (BPU) on dedicated breast positron emission tomography (dbPET). While observing the transverse (**a**), coronal (**b**), and sagittal (**c**) views, a master volume of interest (VOI) (black rectanglar parallelepiped) was placed more than 10 mm away from the image margin (*), excluding the nipple (arrows). SUV_{max} was measured, then the breast tissue was automatically segmented as the region encompassed by a given fixed percent intensity level relative to SUV_{max}. In the segmented VOI (blue), SUV_{mean} and MBV were measured. A threshold equal to 42% of the SUV_{max} was used in this study

In addition, premenopausal participants were classified as having dense or non-dense breasts, and the relationship between BPU and menstrual cycle was analyzed.

The threshold for significance was set at $p < 0.05$. All statistical analyses were conducted using SPSS version 25.0 (IBM Corp, Armonk, NY, USA).

Results

The mean age of all women was 56.3 ± 11.8 years (median 56, interquartile range [IQR] 46–66). Of the 186 women, 98 had mammographically dense breast and 88 had non-dense breast. Of the 59 premenopausal women, 23 were in the menstrual-follicular phase and 36 were in the pre-ovulatory-luteal phase on the day of the dbPET examinations.

In all 186 women, the median values of SUV_{max}, SUV_{mean}, and MBV for the normal breast tissues were 1.78 (IQR 1.54–2.12), 0.96 (IQR 0.79–1.15), and 19.7 cm^3 (IQR 13.0–32.1), respectively. As shown in Fig. 2, age was inversely correlated with SUV_{max} ($p < 0.001$, $r_s = -0.36$) and SUV_{mean} ($p < 0.001$, $r_s = -0.35$) of the normal breast tissues in the Spearman's rank correlation test, while there was no significant correlation between age and MBV ($p = 0.25$, $r_s = -0.085$). Table 1 shows the median SUV_{max}, SUV_{mean}, and MBV of the normal breast tissue according to mammographic density, menopausal status, and menstrual phase on the day of the dbPET examination. The SUV_{max}, SUV_{mean}, and MBV of dense breasts were significantly higher than those of non-dense breasts (all $p < 0.001$). The SUV_{max}, SUV_{mean}, and MBV were significantly higher in premenopausal women than in postmenopausal women ($p < 0.001$, $p < 0.001$, and $p = 0.002$, respectively). In the 59 premenopausal women, the median SUV_{max} of breast tissue in the menstrual-follicular phase was significantly lower than that in the periovulatory-luteal phase ($p = 0.02$). Although not significantly, the SUV_{mean} in the menstrual-follicular phase tended to be lower
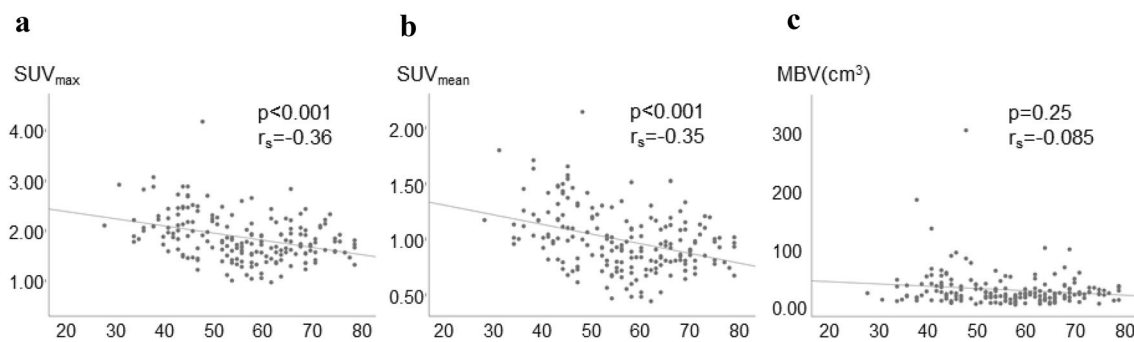

Fig. 2 Scatter diagrams of the correlation of age with SUV_{max} (**a**), SUV_{mean} (**b**), and MBV (**c**) for normal breast tissues

Table 1 Comparison of BPU according to mammographic density, menopausal status, and menstrual phase

	No	SUV_{max}	*P* value	SUV_{mean}	*P* value	MBV	*P* value
Mammographic density			<0.001		<0.001		<0.001
Dense	98	1.99 (1.67–2.30)		1.07 (0.84–1.24)		26.8 (16.4–40.0)	
Non-dense	88	1.65 (1.44–1.88)		0.87 (0.73–1.01)		14.9 (8.2–22.0)	
Menopausal status			<0.001		<0.001		0.002
Premenopause	59	2.08 (1.84–2.44)		1.14 (0.92–1.34)		25.5 (13.6–48.2)	
Postmenopause	127	1.68 (1.50–1.92)		0.88 (0.76–1.05)		18.7 (12.5–28.3)	
Menstrual phase			0.02		0.075		0.900
Menstrual-follicular	23	1.96 (1.63–2.11)		1.06 (0.82–1.19)		23.5 (16.4–41.0)	
Periovulatory-luteal	36	2.11 (1.91–2.58)		1.16 (1.00–1.44)		29.4 (12.3–52.9)	

Data are presented as median (IQR)

BPU background parenchymal uptake, *SUV* standardized uptake value, *MBV* metabolic breast volume

($p = 0.075$) than that in the periovulatory-luteal phase. There was no significant difference in MBV between the menstrual phases ($p = 0.90$).

Stepwise multiple regression analysis for all 186 women revealed that mammographic dense breast and menopausal status independently affected SUV_{max} (both $p < 0.001$), SUV_{mean} (both $p < 0.001$), and MBV ($p = 0.002$, $p = 0.005$, respectively) of the normal breast tissues, whereas age did not emerge as a significant predictor of BPU (Table 2). For the 59 premenopausal women, stepwise multiple regression analysis revealed that dense breast and menstrual phase independently affected SUV_{max} ($p = 0.002$ and, $p = 0.013$, respectively) and SUV_{mean} ($p = 0.002$ and, $p = 0.045$, respectively) of the normal breast tissues, while they were not predictors of MBV (Table 3). Age was not a significant predictor of BPU in premenopausal women.

When we sorted the premenopausal women according to mammographic breast composition, the results in the two groups were different. In 44 premenopausal women with dense breasts, the SUV_{max} and SUV_{mean} of the normal breast tissues in the menstrual-follicular phase were significantly lower than those in the periovulatory-luteal phase ($p = 0.007$ and, $p = 0.038$, respectively), while MBV did not differ significantly ($p = 0.66$) (Fig. 3). In the 15 premenopausal women with non-dense breasts, no statistically significant difference was found between the menstrual-follicular phase and the periovulatory-luteal phase for SUV_{max} ($p = 0.69$) and SUV_{mean} ($p = 0.61$), or MBV ($p = 0.78$).

Discussion

In this study, we showed that the BPU on ring-shaped dbPET was affected by mammographic density, menopausal status, and menstrual phase on the day of the examination. Furthermore, we found that menstrual phase affected BPU, especially in premenopausal women with mammographically dense breasts. To our knowledge, this is the first study to explore the factors affecting the BPU of ring-type dbPET and also the first to investigate the impact of the menstrual cycle on the BPU of dbPET.

Several whole-body FDG PET studies have reported the impact of menopausal status on BPU [4, 5, 12]. In addition, Koo et al. [10] showed that BPU in premenopausal women on PEM was significantly higher than that in postmenopausal women. These results are consistent with those of our study using ring-type dbPET.

Regarding the relationship between BPU and the menstrual cycle, Lin et al. [7] and Park et al. [9] reported that the BPU on whole-body PET in women in the proliferative phase, which is mostly the same as that in the follicular phase, tended to be lower. Our findings using ring-type dbPET were consistent with these findings.

Breast tissue is hormonally sensitive and undergoes cyclic changes during the menstrual cycle. Estrogen and progesterone are representative female hormones that affect the physiological changes in normal breast tissue. Estrogen rises in the late follicular phase and reaches its maximum level immediately before ovulation. During the luteal phase, a

Table 2 Results of multiple regression analysis of independent factors for predicting BPU in all 186 participants

	Viriable	B coefficient	Standardized β coefficient	*P* value	95% confidence interval
SUV_{max}	Dense breast	0.23	0.25	<0.001	0.11 to 0.36
	Menopause	–0.34	–0.34	<0.001	– 0.47 to – 0.20
SUV_{mean}	Dense breast	0.14	0.25	<0.001	0.06 to 0.21
	Menopause	–0.20	–0.34	<0.001	– 0.28 to – 0.12
MBV	Dense breast	14.41	0.23	0.002	5.49 to 23.32
	Menopause	–13.92	–0.21	0.005	– 23.48 to – 4.36

BPU, background parenchymal uptake; SUV, standardized uptake value; MBV, metabolic breast volume

Table 3 Results of multiple regression analysis of independent factors for predicting BPU in 59 premenopausal women

	Viriable	B coefficient	Standardized β coefficient	*P* value	95% confidence interval
SUV_{max}	Dense breast	0.45	0.38	0.002	0.17–0.73
	Periovulatory-luteal	0.32	0.30	0.013	0.069–0.56
SUV_{mean}	Dense breast	0.27	0.38	0.002	0.10–0.44
	Periovulatory-luteal	0.16	0.24	0.045	0.001–0.31

BPU background parenchymal uptake, *SUV* standardized uptake value, *MBV* metabolic breast volume
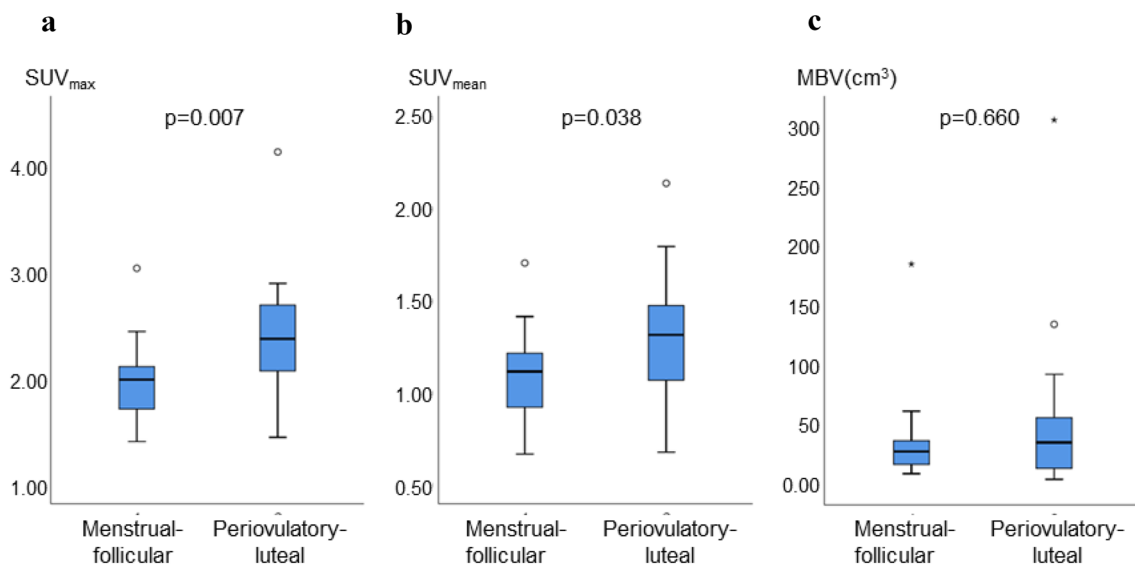
Fig. 3 SUV_{max} (**a**), SUV_{mean} (**b**), and MBV (**c**) of normal breast tissues in 44 premenopausal women with dense breast. SUV_{max} and SUV_{mean} of normal breast tissues in the menstrual-follicular phase were significantly lower than those in the periovulatory-luteal phase (**a**), (**b**), while MBV did not differ significantly (**c**)

small peak in estrogen levels is noted, and at this time, a prominent peak in progesterone levels appears. For histological changes in breast tissues, variable vacuolation of breast epithelial cells, increased vasodilation, and permeability and swelling of adjacent fibrous tissues are explained by the effect of estrogen [13–15]. In contrast, maximum proliferation of luminal epithelial cells is observed during the luteal phase, which is positively correlated with serum progesterone levels [16]. Previous reports have suggested that mitotic activity in the breast lobules may be increased by progesterone [17, 18], and that epithelial proliferation may occur due to the synergic effect of high levels of estrogen and progesterone [19, 20]. Although it is difficult to clarify the mechanism of physiological change of FDG uptake in the breast, we hypothesize that epithelial proliferation activated by estrogen and progesterone under the menstrual cycle may correlate with increased glucose metabolic activity. Consequently, as these hormone levels are low during the follicular phase, except near ovulation, BPU might also be low in this phase. Postmenopausal women may have lower BPU than premenopausal women due to less exposure to these female hormones.

Several previous studies reported that breast mammographic density correlated with BPU on whole-body PET or PEM [4, 5, 10, 12], and the present results using ring-shaped dbPET agree with them. Further, in the current study, the SUV_{max} and SUV_{mean} of normal breast tissues were significantly different between the menstrual-follicular phase and the periovulatory-luteal phase in premenopausal women with dense breasts, but not in women with non-dense breasts. It is difficult to determine why the results of BPU

changes differ between non-dense and dense breasts, but it can be hypothesized that dense breasts may have a greater amount of stroma and may be more susceptible to variations in hormone levels during the menstrual cycle. Further research is required to elucidate the biological mechanisms underlying elevated BPU levels.

On the other hand, MBV was not correlated with breast density in premenopausal women in this study. Breast density represents the morphological breast composition on mammography, not its metabolism. If the entire morphological fibroglandular breast tissue is included in the MBV estimation, the segmentation threshold may vary depending on the characteristics of the breast tissue, such as breast density. Another possible reason explaining the result is a specific disadvantage of dbPET, namely that the breast tissue near the chest wall is likely to be out of the field, in the so-called the blind area [21, 22]. As many Japanese women breast have less fat component, their fibroglandular tissues are often located near the chest wall, even when they are in the prone position. This tendency is particularly common in young women with less fat component who are less likely to have breast ptosis [23]. In the present study, MBV may have been underestimated, in particular in premenopausal women with dense breasts and less fat, as the fibroglandular tissue near the chest wall was out of the field of dbPET imaging.

Based on the results of our study, it may be advisable to avoid scheduling dbPET scans during the periovulatory-luteal period. However, before we can do this, we need to clarify the impact of the BPU of dbPET on breast cancer diagnosis in actual clinical applications. Owing to its high spatial resolution, dbPET has shown higher sensitivity than

whole-body PET for the detection, in particular, of sub-centimetric small cancers [24]. Additionally, Sato et al. have demonstrated, using a phantom, that the contrast with background was much higher in dbPET than in the PET/CT image [28]. Thus, considering these, we hypothesize that the diagnostic impact of BPU on dbPET may be less severe than on whole-body PET. To further investigate these issues, clinical case-based studies are needed. On the other hand, it may be useful to schedule dbPET examinations for women with dense breasts according to the menstrual cycle.

This study has some limitations. First, it was a retrospective study from a single institution, and larger studies are required to validate the results. Second, BPU measurements were performed by a single operator, so that reproducibility and consistency have not been verified. Segmentation of breast tissue was performed automatically by threshold setting; however, primary placement of the master VOI was done manually, so as to include the entire breast tissue, more than 10 mm away from the image margin, and excluding the nipple: Such procedures can involve some arbitrariness and may depend on the experience of the examiner. Third, SUV_{mean} and MBV were defined, respectively, as the average SUV of voxels and the total volume of voxels within the VOI exceeding 42% of the SUV_{max}. We have not verified whether this threshold setting was valid. Fourth, as mentioned above, in ring-shaped dbPET, the area from the bed to the upper edge of the detector becomes a blind area, and the breast tissue residing in the deep part cannot be evaluated. In addition, the noise generated on the chest wall can affect the measurement of the SUV.

In conclusion, our analysis demonstrates that FDG uptake in normal breast tissues using ring-shaped dbPET is associated with mammographic density, menopausal status, and menstrual cycle. Furthermore, menstrual cycle was significantly associated with BPU, especially in premenopausal women with mammographically dense breasts. Although further research is needed, it may be advisable to schedule the dbPET imaging examination with considering the patient's menstrual cycle.

Declarations

References

1. García Hernández T, Vicedo González A, Ferrer Rebolleda J, Sánchez Jurado R, Roselló Ferrando J, Brualla González L, et al. Performance evaluation of a high resolution dedicated breast PET scanner. Med Phys. 2016;43:2261.

2. Nishimatsu K, Nakamoto Y, Miyake KK, Ishimori T, Kanao S, Toi M, et al. Higher breast cancer conspicuity on dbPET compared to WB-PET/CT. Eur J Radiol. 2017;90:138–45.

3. Fowler AM. A molecular approach to breast imaging. J Nucl Med. 2014;55:177–80.

4. Vranjesevic D, Schiepers C, Silverman DH, Quon A, Villalpando J, Dahlbom M, et al. Relationship between ^{18}F-FDG uptake and breast density in women with normal breast tissue. J Nucl Med. 2003;44:1238–42.

5. Zytoon AA. Standardized uptake value variations of normal glandular tissue at dual time point FDG-PET/CT imaging. Int J Med Imaging. 2013;1:56–65.

6. Mavi A, Cermik TF, Urhan M, Puskulcu H, Basu S, Cucchiara AJ, et al. The effect of age, menopausal state, and breast density on ^{18}F-FDG uptake in normal glandular breast tissue. J Nucl Med. 2010;51:347–52.

7. Lin CY, Ding HJ, Liu CS, Chen YK, Lin CC, Kao CH. Correlation between the intensity of breast FDG uptake and menstrual cycle. Acad Radiol. 2007;14:940–4.

8. An YS, Jung Y, Kim JY, Han S, Kang DK, Park SY, et al. Metabolic activity of normal glandular tissue on ^{18}F-Fluorodeoxyglucose positron emission tomography/computed tomography: correlation with menstrual cycles and parenchymal enhancements. J Breast Cancer. 2017;20:386–92.

9. Park H-H, Shin JY, Lee JY, Jin GH, Kim HS, Lyu KY, et al. Discussion on the alteration of ^{18}F-FDG uptake by the breast according to the menstrual cycle in PET imaging. Annu Int Conf IEEE Eng Med Biol Soc. 2013;2013:2469–72.

10. Koo HR, Moon WK, Chun IK, Eo JS, Jeyanth JX, Chang JM, et al. Background ^{18}F-FDG uptake in positron emission mammography (PEM): correlation with mammographic density and background parenchymal enhancement in breast MRI. Eur J Radiol. 2013;82:1738–42.

11. Erdi YE, Mawlawi O, Larson SM, Imbriaco M, Yeung H, Finn R, et al. Segmentation of lung lesion volume by adaptive positron emission tomography image thresholding. Cancer. 1997;80(Suppl):2505–9.

12. Lakhani P, Maidment ADA, Weinstein SP, Kung JW, Alavi A. Correlation between quantified breast densities from digital mammography and ^{18}F-FDG PET uptake. Breast J. 2009;15:339–47.

13. Christov K, Chew KL, Ljung BM, Waldman FM, Duarte LA, Goodson WH 3rd, et al. Proliferation of normal breast epithelial cells as shown by in vivo labeling with bromodeoxyuridine. Am J Pathol. 1991;138:1371–7.

14. Longacre TA, Bartow SA. A correlative morphologic study of human breast and endometrium in the menstrual cycle. Am J Surg Pathol. 1986;10:382–93.

15. Ramakrishnan R, Khan SA, Badve S. Morphological changes in breast tissue with menstrual cycle. Mod Pathol. 2002;15:1348–56.

16. Brisken C, Hess K, Jeitziner R. Progesterone and overlooked endocrine pathways in breast cancer pathogenesis. Endocrinology. 2015;156:3442–50.

17. Speroff L. Role of progesterone in normal breast physiology. J Reprod Med. 1999;44(Suppl):172–9.

18. Chang KJ, Lee TT, Linares-Cruz G, Fournier S, de Ligniéres B. Influences of percutaneous administration of estradiol and progesterone on human breast epithelial cell cycle in vivo. Fertil Steril. 1995;63:785–91.

19. Pike MC, Spicer DV, Dahmoush L, Press MF. Estrogens, progestogens, normal breast cell proliferation, and breast cancer risk. Epidemiol Rev. 1993;15:17–35.

20. Navarrete MAH, Maier CM, Falzoni R, de Quadros LGA, Lima GR, Baracat EC, et al. Assessment of the proliferative, apoptotic and cellular renovation indices of the human mammary epithelium

during the follicular and luteal phases of the menstrual cycle. Breast Cancer Res. 2005;7:R306–13.

21. Satoh Y, Kawamoto M, Kubota K, Murakami K, Hosono M, Senda M, et al. Clinical practice guidelines for high-resolution breast PET, 2019 edition. Ann Nucl Med. 2021;35:406–14.

22. Satoh Y, Motosugi U, Imai M, Omiya Y, Onishi H. Evaluation of image quality at the detector's edge of dedicated breast positron emission tomography. EJNMMI Phys. 2021;8:5.

23. Satoh Y, Motosugi U, Imai M, Onishi H. Comparison of dedicated breast positron emission tomography and whole-body positron emission tomography/computed tomography images: a common phantom study. Ann Nucl Med. 2020;34:119–27.

24. Sueoka S, Sasada S, Masumoto N, Emi A, Kadoya T, Okada M. Performance of dedicated breast positron emission tomography in the detection of small and low-grade breast cancer. Breast Cancer Res Treat. 2021;187(1):125–33.

Authors and Affiliations

Yuri Shimizu[1] · Hiroko Satake[1] · Satoko Ishigaki[1] · Kazuhiro Shimamoto[2] · Fuga Uota[1] · Masanori Tadokoro[3] · Tomohiro Sato[3] · Katsuhiko Kato[4] · Tsuneo Ishiguchi[3] · Shinji Naganawa[1]

1 Department of Radiology, Nagoya University Graduate School of Medicine, 65 Tsurumai-cho, Showa-ku, Nagoya, Aichi 466-8550, Japan

2 Nagoya Jhohoku Radiology Clinic, 1-7-23 Heian, Kita-ku, Nagoya, Aichi, Japan

3 Trust Clinic, 1-30-22 Sakae, Naka-ku, Nagoya, Aichi, Japan

4 Department of Radiological and Medical Laboratory Sciences, Nagoya University Graduate School of Medicine, 1-1-20 Daiko-Minami, Higashi-ku, Nagoya, Aichi, Japan